International Journal of Pharmaceutics 673 (2025) 125384

Contents lists available at ScienceDirect

International Journal of Pharmaceutics

journal homepage: www.elsevier.com/locate/ijpharm

Spray drying of an oil-in-water emulsion containing vitamin D3: a synergy between formulation and process conditions to obtain microparticles

Giada Diana [a,1], Andrea Milanesi [a,b,1], Alessandro Candiani [a], Alessandro Sodano [b], Paolo Rassè [b], Andrea Foglio Bonda [b], Laura Alessandroni [c], Lorella Giovannelli [a,b], Lorena Segale [a,b,*], Jean Daniel Coïsson [a]

[a] Department of Pharmaceutical Sciences, University of Piemonte Orientale, Largo Donegani 2, 28100 Novara, Italy
[b] APTSol Srl - Largo Donegani 2, 28100 Novara, Italy
[c] School of Pharmacy, Chemistry Interdisciplinary Project (ChIP), University of Camerino, Via Madonna delle Carceri, 62032 Camerino, Italy

ARTICLE INFO

Keywords:
Vitamin D3
Emulsion
Microparticles
Spray drying
Pilot-scale

ABSTRACT

Spray drying is a practical solution to convert oil-in-water emulsion into solid microparticles. In this work, a formulation study was conducted to identify the best composition of vitamin D3-loaded oil-in-water emulsion to process via a lab-scale spray dryer. The emulsion was composed of vitamin D3 oily solution (7 % w/w) and maltodextrin (21 % w/w), arabic gum (9 % w/w) and pea protein hydrolysate (1 % w/w) aqueous solution and was characterized by optimal stability (> 24 h). The spray drying process (T_{in}: 160 °C; T_{out}: 94 °C; Gas atomization: 1.75 bar; Feeding rate: 8.75 g/min) was successful: the process yield was good, and the obtained powder had an acceptable residual humidity. The average diameter of microparticles was 23 μm with a quite wide particle size distribution. The oil and vitamin D3 recovered from the powder were 85.69 ± 3.91 % and 80.10 ± 9.94 % of the expected, respectively. The accelerated stability and photostability study results showed that the percentage of vitamin D3 present in the powder after storage was twice compared to vitamin D3 in oil solution stored at the same conditions. Moreover, the scale-up of the process from lab- to pilot-scale spray dryer was encouraging. Regardless of the top or bottom spray set-up, the pilot scale treatments increased the production rate and improved drying efficiency. The top spray configuration and a low inlet temperature guaranteed a yield of over 86 %, about 3 % residual humidity in the powder, and preserved the oil quality, maintaining a peroxide value comparable to the initial one.

1. Introduction

Vitamin D3 is a liposoluble compound in which there is a lot of interest nowadays because its high deficiency and insufficiency are a global health issue that afflicts more than one billion children and adults worldwide (Pludowski et al., 2024). Various approaches to developing new medicinal or nutraceutical products for the delivery of vitamin D3 are evaluated by the researchers (Maurya et al., 2020). Terracina et al. (2022) proposed spray drying to produce gastro-resistant microparticles containing liposoluble vitamins using a suspension as feed liquid to submit to the spray drying process. The obtained results demonstrated the effect of the formulation composition to control the release profiles of some model lipid vitamins, but the process yields in the case of vitamin D3 didn't exceed 57 %. Dima et al. (2020) described spray-dried vitamin D3 microparticles obtained from an oil-in-water emulsion where arabic gum and chitosan were used as carrier excipients. In this case, the encapsulation efficiency was good, but a low production yield, caused by the high adhesion properties of chitosan, characterized the spray drying process. Moreover, there is an increasing interest in co-encapsulating vitamin D3 with other active compounds for food fortification using spray drying technique (Bajaj et al., 2021; Tchuenbou-Magaia et al., 2022).

The formulation of vitamin D3 in solid oral delivery systems can represent a challenge because of its low solubility in water and, consequently, in physiological fluids, which is responsible for its low bioavailability. Moreover, this task can become even more difficult because vitamin D3 is a photo and thermosensitive compound.

Oil-in-water (O/W) emulsion, an appropriate dosage form for

* Corresponding author at: Largo Donegani 2, 28100 Novara, Italy.
E-mail address: lorena.segale@uniupo.it (L. Segale).
[1] These authors contributed equally to this work.

https://doi.org/10.1016/j.ijpharm.2025.125384
Received 2 December 2024; Received in revised form 20 February 2025; Accepted 20 February 2025
Available online 20 February 2025

overcoming the poor oral bioavailability of lipophilic active substances, combined with the advantages of the spray drying process, could represent a promising solution to better preserve the encapsulated active compound. Spray drying can easily convert O/W emulsions into powders, improving the final product's quality, shelf-life, handling, and storage. The result is the production of solid, stable microcapsules with a heterogeneous polynucleate structure in which numerous small lipophilic cores are embedded in a hydrophilic matrix (Salama, 2020).

The selection of carrier excipients with performing emulsifying properties and film-forming ability and their combination at defined concentration is fundamental to have a starting emulsion with suitable stability, viscosity, and droplet size distribution. In this way, the oil droplets in which the active substance has been dissolved could be better retained during spray drying, enhancing the effectiveness of the encapsulation process (Carneiro et al., 2013). Still, the success of the spray drying treatment can only be achieved if appropriate process parameters are also selected. The inlet temperature of the drying gas (T_{in}) and, consequently the outlet temperature (T_{out}), affects some aspects strictly correlated with the quality of the final product: residual humidity of the powder, responsible for eventual microbial contamination, and product stickiness and/or the stability of the spray-dried active compound if it is sensitive to thermal treatment (Milanesi et al., 2022).

In developing new spray-dried products, laboratory-scale results are insufficient to guarantee a successful transfer to industrial production. Scaling up the process is mandatory to understand how to preserve the technological characteristics and quality of the obtained powders on a large scale. However, the amounts of raw material and the samples required for research tests are relatively low. For this reason, in the starting phase, it is more convenient to work with a small-scale or pilot spray dryer to prevent product waste and scale-up risks (Poozesh and Bilgili, 2019). In the literature, there are several examples of the treatment of oil-in-water emulsions via spray drying to obtain dried powders (Gonçalves et al., 2022; Mohammed et al., 2020) but the combination of this aim with the study of the most adequate process conditions and equipment configuration to use for transferring the spray drying process from a lab-scale to a pilot-scale is not so common. This research aimed to produce vitamin D3-loaded solid microparticles by spray drying technology, preserving the stability of this lipophilic active compound. In detail, this project focused on the formulation of O/W placebo emulsions characterized by adequate stability and viscosity to be processed by spray drying and the identification of the best spray drying process parameters using a small-scale spray dryer to obtain dried microparticles with good technological properties. The selected formulation was then enriched with vitamin D3 and submitted to spray drying using the optimal process conditions to evaluate its suitability in preserving the lipophilic compound. Moreover, a pilot-scale spray dryer was used for the treatment of O/W placebo emulsion to evaluate the most suitable equipment configuration and the most promising processing parameters to maintain the quality of the encapsulated oil.

2. Materials and methods

2.1. Materials

Vitamin D3 was provided by Alfa Aesar (Thermo Fisher GmbH, Kandel, Germany). Edible sunflower oil (Bellasan) was acquired in a local market. Maltodextrin ($16 < DE < 19.9$) was purchased from A.C.E. F. (Fiorenzula D'Arda, Italy). Arabic gum, soy protein, rice starch and carrageenan λ were provided by Farmalabor (Canosa di Puglia, Italy). Pea protein hydrolysate was kindly donated by A. Costantino & C. Spa (Favria, Italy). All other reagents were of analytical grade and used as received.

2.2. Experimental methods

2.2.1. Formulation study

2.2.1.1. Preparation of O/W emulsion. The preliminary work started with the formulation of O/W placebo emulsions, whose dispersed phase was sunflower oil and the continuous phase a maltodextrin water solution. As reported in Table 1, the O/W emulsions were similar in terms of the final vegetable oil content and maltodextrin concentration, while they differed in the type of natural emulsifier tested: soy protein (E1), rice starch (E2), pea protein hydrolysate (E3), carrageenan λ (E4). The emulsifier was dissolved in the aqueous phase and the two phases were emulsified by Ultra-Turrax® (16,000 rpm) for five minutes.

The most promising O/W placebo emulsion with regard to physical stability and viscosity was selected as the starting point for formulation improvement, in which the emulsifier percentage was increased and arabic gum was added as wall material. Then, vitamin D3 (0.1 % w/w) was solubilized in the oil phase of the optimized O/W emulsion (E5) prepared according to the procedure described above and the resulting emulsion was coded vitD-E5 (Table 1).

2.2.1.2. Appearance evaluation, physical stability and viscosity analysis. All placebo emulsions were observed by optical microscopy (Stereomicroscope Leica-S9i, Wetzlar, Germany) immediately after their preparation.

The physical stability of the O/W placebo emulsions was evaluated by pouring an aliquot of each sample into a glass tube maintained at room temperature. Each sample was observed and photographed after 15, 30, 60, and 120 min to assess the potential phase separation.

Viscosity analysis was performed on the O/W emulsions reconsidered for formulation improvement based on their appearance and stability and on the optimized O/W emulsion (E5). The viscosity was measured at 25 °C using a Brookfield viscometer (Brookfield Programmable DV-II Viscometer) equipped with S18 spindle set to 35 rpm.

2.2.1.3. Droplet size distribution (DSD). The droplet size distribution of the optimized placebo emulsion (E5) was evaluated using laser diffraction technology (Bettersizer 2600, Bettersize Instruments, Munich, Germany) with wet dispersion equipment (BT-802) and water as medium. The analysis was carried out by adding the sample drop by drop directly into the vessel. The stirring speed was set at 600–800 rpm, and the ultrasound was switched off. Results are reported as the average diameter of droplets (D [4,3]) and as Dv10, Dv50 and Dv90 values.

2.2.2. Lab-scale spray drying

The O/W emulsions (about 50 g) with and without vitamin D3, prepared as described above, were submitted to lab-scale spray drying treatment using a Buchi Mini Spray Dryer B-290 equipped with a high-performance cyclone, a nozzle with a 0.7 mm tip hole and 1.5 mm cap hole, and a dehumidifier (Buchi dehumidifier B-296®) for the airflow. At the end of the process, all the batches of powders were recovered and packaged in a closed polypropylene Falcon tube.

These spray drying tests were performed on the most appropriate

Table 1
Percentage composition (w/w) of O/W emulsions tested.

Components	E1	E2	E3	E4	E5	vitD-E5
Maltodextrin	20.0	20.00	20.0	20.0	21.0	21.0
Arabic gum	––	––	––	––	9.0	9.0
Water	72.5	72.5	72.5	72.5	62.0	62.0
Soy protein	0.5	––	––	––	––	––
Rice starch	––	0.5	––	––	––	––
Pea protein hydrolysate	––	––	0.5	––	1.0	1.0
Carrageenan λ	––	––	––	0.5	––	––
Sunflower oil	7.0	7.0	7.0	7.0	7.0	6.993
Vitamin D3	––	––	––	––	––	0.007

emulsion among E1, E2, E3, and E4 to evaluate the process feasibility. The treatment was carried out with T_{in} of 130 °C, T_{out} of about 80 °C (a target outlet temperature to limit product degradation), 100 % aspiration, 1.75 bar of gas atomization, and 7 % pump (feeding rate 3.55 g/min).

Moreover, four microparticle batches (P1, P2, P3, P4) were produced starting from E5 by changing the spray drying process parameters, as reported in Table 2.

The process conditions used to obtain P4 powders were also set for the treatment of the vitD-E5 emulsion without light exposure and covering the entire spray dryer to preserve the photosensitive compound.

The percentage process yields PY (%) were calculated using Equation (1). The "weight of actual powder" represented the weight of the collected powder, and the "weight of theoretical powder" was the sum of the weight of the solids and oil included in the formulation.

$$\text{PY}\,(\%) = \frac{\textit{Weight of actual powder}}{\textit{Weight of theoretical powder}}\ x100 \quad (1)$$

2.2.3. Pilot-scale spray drying tests

2.2.3.1. Spray drying equipment and process parameters. The E5 emulsion (about 10 kg) was treated using a pilot-scale spray dryer, that is APT 5.0 + spray dryer (APTSol S.r.l., Novara, Italy) equipped with a two-fluid nozzle with internal mixing and characterized by a tip of 1.2 mm. Two different machine configurations were used: co-current (top spray set-up, the batches were coded T1 and T2) and counter-current (bottom spray set-up, the batches were coded B1 and B2). At first, the T_{in} was kept constant (130 °C) to easily compare the results obtained according to the different configurations, the a-dimensional parameter (ADP) was considered as a starting strategy to find suitable drying conditions in the pilot scale (Milanesi et al., 2022). Moreover, it was decided to evaluate the impact of the variation of T_{in} while maintaining constant equipment set-up. The process parameters are summarized in Table 3.

2.2.4. Characterization

2.2.4.1. Oil recovery. A liquid–liquid extraction was carried out to recover the sunflower oil from the powder obtained via spray drying. Precisely, about 1 g of collected powder from the preliminary lab-scale spray drying test was rehydrated in 20 mL of deionized water, and then the resulting emulsion was transferred into a separatory funnel, and n-hexane was added as lipophilic solvent (1:1 solvent:emulsion). After vigorous shaking, a phase separation between aqueous dispersion and hexane from the bottom to the top was visible. The hexane phase containing the sunflower oil was removed from the top of the funnel and restored with fresh n-hexane (20 mL) and the entire process was repeated three times. The n-hexane phase recovered was introduced into a rotary evaporator (Buchi, Rotavapor R-210 equipped with heating bath B-491 and vacuum pump V-700) to remove the organic solvent. The residual oil was gravimetrically quantified.

In the case of the powders obtained from the spray drying treatments of E5 (P1, P2, P3 and P4, T1, T2, B1 and B2) and of vitD-E5, the liquid–liquid extraction method was slightly modified compared to that described above because the presence of arabic gum limited the release of oil droplets from the powder and the emulsion reconstitution. 1 g of the collected powder was added to 20 mL of deionized water and maintained under stirring until the rehydration process was complete and the emulsion was reconstituted. Then, the stirring was stopped to let the phase separate. The oil was subsequently recovered by a liquid–liquid extraction using n-hexane as lipophilic solvent (40 % more than the emulsion volume) and acetone (1:1 solvent:emulsion) as an aid for the oil droplets recovery, making the arabic gum rapidly gelled and squeezed.

Table 2
Process parameters of lab-scale spray drying treatments.

	P1	P2	P3	P4
T_{in} (°C)	130	130	130	160
T_{out} (°C)	87	84	82	85
Aspiration (%)	100	100	100	100
Gas atomization (bar)	1.75	1.75	1.75	1.75
Pump (%)	7	12	14	26
Feeding rate (g/min)	2.46	3.70	5.46	8.75

Table 3
Process parameters of pilot-scale spray drying treatments.

	T1	B1	T2	B2
T_{in} (°C)	130	130	170	210
T_{out} (°C)	74–75	74–75	85.6	108.3
Gas atomization (bar)	1.20	1.20	1.20	1.20
Feeding rate (g/min)	45	45	45	45

The percentage of the encapsulated oil was calculated following Equation (2), considering the extracted oil compared to the expected oil from a precise weight of powder.

$$\text{Oil}\,(\%) = \frac{\textit{Weight of extracted oil}}{\textit{Weight of expected oil}}\ x100 \quad (2)$$

2.2.4.2. Residual water. The percentage of residual water in the collected powders was determined by a thermobalance (Radwag—Ma50/1.R.WH) by analyzing the variation in the sample weight imputable to the water evaporation. A low amount of sample was introduced into the balance's weighing pan, and the temperature was gradually increased to 125 °C, maintained until the sample weight was constant. The collected results are reported as the percentage of weight loss by the sample during the analysis compared to its initial. The analysis was repeated three times for each sample.

2.2.4.3. Bulk and tapped density. The bulk density (ρ_b) of the powders recovered from the lab-scale and pilot-scale spray dryer was assessed by gently filling a graduate cylinder with a precise amount of powder (about 10 g) without compaction and reading directly the apparent volume (V_0). The bulk density was calculated according to Equation (3). To determine the tapped density (ρt), the cylinder was tapped manually until no variation in the powder volume was evident. That volume was the tapped volume (V_f) and was used to calculate the tapped density according to Equation (4).

$$\text{Bulk density}\,(\rho_b) = m/V_0 \quad (3)$$

$$\text{Tapped density}\,(\rho_t) = m/V_f \quad (4)$$

The flowability of the dried microparticles obtained from the lab-scale and pilot-scale spray dryer was established according to the Hausner ratio (HR) values calculated using bulk and tapped density (Council of Europe - EDQM, 2023) and the following Equation (5). The results were expressed as the mean of three determinations ± standard deviation.

$$\text{Hausner ratio}\,(\text{HR}) = \frac{\rho_t}{\rho_b} \quad (5)$$

2.2.4.4. Particle size distribution. The particle size distribution of the collected powders was evaluated by laser diffraction technology (Bettersizer 2600, Bettersize Instruments, Munich, Germany) with dry dispersion equipment working 0.15 MPa (BT-903). Results are reported as the average diameter of particles (D [4,3]), Dv10, Dv50, and Dv90 values, which indicate the diameter of the 10 %, 50 % and 90 % of the particles, and SPAN index for the evaluation of the width of particle size distribution, calculated according to Equation 6:

SPAN = (Dv90 – Dv10)/Dv50 Eq. (6).

2.2.4.5. Determination of oil peroxide value and oxidative stability. The peroxide value of the fresh sunflower oil and the oil extracted from the powders was evaluated by the spectrophotometric method thanks to the ability of hydroperoxides to oxidize ferrous ions (Fe^{2+}) to ferric ions (Fe^{3+}) in an acidic medium (Candiani et al., 2023). Precisely, an exact weighed amount of oil sample (between 0.01 and 0.02 g) was introduced into a vial and 9.9 mL chloroform–methanol (7:3, v/v) mixture, 50 μL ammonium thiocyanate solution (30 % w/w) and 50 μL of iron (II) chloride solution (2 mg/mL acidified with 10 M HCl) were added and mixed. The samples were kept at room temperature for 5 min to promote the reaction and then the absorbance of the sample was determined spectrophotometrically at 500 nm (Shimadzu UV-1900).

Moreover, the powders obtained from pilot-scale spray drying were submitted to a stability study to evaluate the impact of storage conditions on the oil quality. Each sample was kept in a sealed bag at room temperature and away from the light source. To investigate the polymeric matrix's preserving ability, a small amount of untreated sunflower oil was kept in the same conditions and used as reference. All the samples were analyzed in terms of peroxide value after six months of storage.

The results were reported as a mean of three determinations.

2.2.4.6. Determination of vitamin D3 content. In the case of microparticles obtained by spray drying of vitD-E5 emulsion, the vegetable oil was recovered starting from the powder according to the same method described above and vitamin D3 was isolated from the extracted oil by solid-phase extraction according to the procedure described by Candiani et al., 2023. At the same time, vitamin D3 was also recovered from the freshly prepared oil solution (0.1 % w/w) to evaluate the efficiency of the method. The recovered vitamin D3 was dissolved in 1 mL methanol, the solution diluted 1:40 and analyzed by HPLC-DAD following the method described and validated by Candiani et al. (2023) (Shimadzu LC-20A Prominence chromatographic system, diode array detector SPD-M20A at 265 nm; reversed-phase Kinetex C-18 100 Å LC Column (50 × 2.1 mm i.d., 5 μm); eluent A: water/formic acid 0.1 % v/v and eluent B: acetonitrile/formic acid 0.1 % v/v). Moreover, the vitamin D3 recovery was also determined from a vitamin oily solution (0.1 % w/w) directly exposed at the same temperature used as T_{in} during spray drying treatment, to assess the thermal stability of the active compound.

2.2.4.7. Stability study. The vitamin D3 oily solution and the powder obtained from the spray drying treatment of vitD-E5 emulsion were stored, in well-closed amber vials, in a climatic chamber at 40 °C and 75 % relative humidity (RH) for six months to evaluate the stability of vitamin D3 (ICH Topic Q1A (R2), 2003).

The photostability of vitamin D3 in oily solution and loaded into powders was evaluated after exposure of the sample to a UV light lamp (FOTO/UV 26 Transilluminator, Fotodyne, Hartland, USA) of 21 x 26 cm of viewing surface and four 8-watt 312 nm bulbs for 240 sec (dose: 14.07 J/cm^2) according to the ICH requirements (ICH Topic Q1B, 1998).

Oil recovery from the powder and vitamin D3 extraction from the oily solutions were carried out as described above. The same method reported in paragraph 2.2.4.6 was adopted to quantify vitamin D3.

2.2.4.8. SEM analysis. The powder obtained under the best process conditions of pilot-scale tests according to the oil quality was submitted to a detailed morphological investigation using scanning electron microscopy (SEM) (Phenom XL, Thermo-Fischer Scientific, Waltham, MA, USA) at 15 kV voltage without gold coating of the particle's external surface.

2.2.5. Statistical analysis

All the data were expressed as the mean of three determinations ± standard deviation. Statistical analysis was carried out with one-way analysis of variance (ANOVA), followed by the post hoc Tukey test using R studio (version 4.4.1. for Windows) (Studio, PBC, Boston, USA) to investigate the differences between groups. The statistical significance level was set at 0.05.

3. Results and discussion

3.1. Formulation study

3.1.1. Preliminary work

The first part of this study involved the formulation of an O/W placebo emulsion characterized by adequate stability and viscosity to be processed by spray drying. Four different natural emulsifiers were tested. Immediately after the preparation (t0), E1 and E2 were coarse and inhomogeneous emulsions, while the oil phases of E3 and E4 appeared well dispersed, as demonstrated by the stereomicroscope images (Fig. 1). E1 and E2 separated immediately, while E3 was more stable than E1 and E2 but less stable (15 min) than E4 (more than 2 h) (Fig. 2). The emulsifier included in E4 formulation, that is carrageenan, preserved the stability of the system thanks to its predisposition to increase the viscosity of the preparation (Pacheco-Quito et al., 2020).

The stability of an emulsion to be treated by spray drying must be maintained throughout the process.

For this reason, among the formulated placebo emulsions, only E4 was submitted to a preliminary spray drying test to prove the process's feasibility. The process yield was 72.40 %, but a great amount of oil was lost on the tower walls. The oil loaded into microparticles was about 30 % of the expected. These results were not satisfying and demonstrated that the selected wall material was inadequate. Maltodextrin alone was probably not able to act as a carrier. Thus, the optimization of the starting emulsion formulation occurred.

3.1.2. Optimization phase

Among the emulsions tested in the preliminary step, E1 and E2 were discarded because they were unstable, while E3 and E4 were reconsidered for formulation improvement after the evaluation of their viscosity, a parameter that strongly affects the feasibility and the outcome of the spray drying process (Camacho-Lie et al., 2023). The viscosity of E3 and E4 was 8.48 cP and 72.00 cP, respectively. Considering that a low starting viscosity allowed the addition of other excipients to the formulation even if they are characterized by thickening properties without compromising the efficiency of the spray drying process (Esposito et al., 2020; O'Sullivan et al., 2019), E3 emulsion was selected as the starting point for formulation improvement. The E3 emulsion formulation was modified increasing the percentage of pea protein hydrolysate from 0.5 to 1.0 % and using as wall material not only maltodextrin but also arabic gum, selected for its emulsifier and film-forming properties. The mixture of these two carrier excipients can stabilize the emulsion and the distribution of its droplet size and, at the same time, improve the encapsulation efficiency (Mohammed et al., 2020). Moreover, the presence of pea protein hydrolysate as an emulsifier was promising, being this excipient non-allergenic, characterized by high nutritional value and antioxidant properties potentially able to reduce oil oxidation of spray dried emulsions (Tamm et al., 2016; van Boven et al., 2024).

The optimized emulsion, coded E5, had adequate characteristics to be treated by spray drying (both at a lab-scale and a pilot-scale): viscosity of 73 cP, physical stability for more than 24 h and 38 % total solid content (oil + maltodextrin + arabic gum + pea protein hydrolysate) in line with the percentages reported in the literature (Carmona et al., 2018).

E5 emulsion was characterized by a homogenous dispersion of small oil droplets, as shown in the stereomicroscope image (Fig. 3), whose mean diameter was 2.03 μm with Dv10 = 1.104 μm; Dv50 = 2.448 μm and Dv90 = 4.944 μm. This can be surely considered a promising result

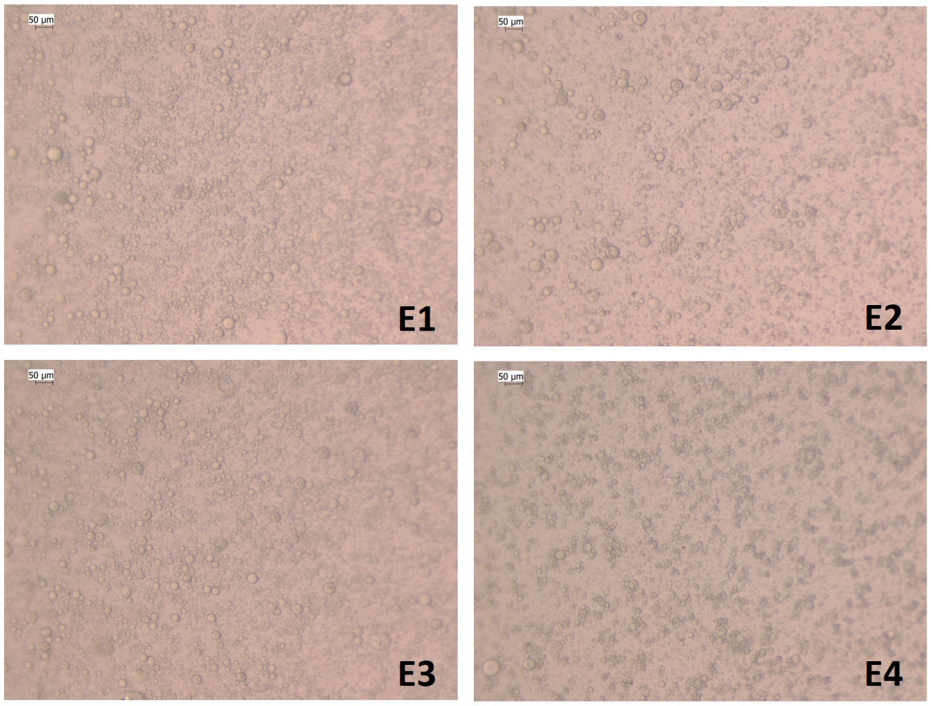

Fig. 1. Stereomicroscope images of emulsions just prepared (t0).

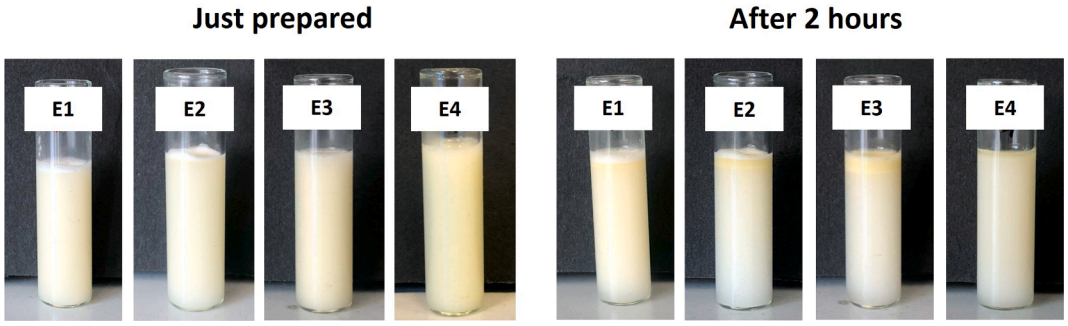

Fig. 2. Images of emulsions just prepared and after 2 h.

Fig. 3. Stereomicroscope image of E5 emulsion immediately after the preparation.

for the next steps of the work, as the microencapsulation process by spray drying may be more successful using an emulsion with small droplet dimensions as feed material (Tonon et al., 2011).

3.2. Lab-scale spray-dried powders

Four microparticle batches were produced starting from E5 using different spray drying process parameters. The powders coded P1, P2, and P3 were obtained by maintaining T_{in} constant and gradually increasing the feeding rate that was necessarily responsible for a decrease in T_{out}. On the other hand, P4 powder was produced by simultaneously increasing T_{in} and the feeding rate to evaluate the effect of exposing the feed emulsion to a higher temperature, still guaranteeing low levels of residual water in the final product.

The process yields of the four batches of microparticles were almost similar (Table 4) and relatively high compared to the data reported in the literature for the yield of a lab-scale spray drying treatment (Al-Khattawi et al., 2018; Poozesh and Bilgili, 2019). In detail, they were about 86 % for P1, P2, and P3 and slightly higher (about 89 %) in the case of P4. The latter result can be explained by considering the highest T_{in} (160 °C, Table 2)) selected for the production of P4 powder, which caused a more efficient transfer of mass and heat (Sablania and Bosco,

Table 4
Characteristics of lab-scale spray-dried powders. Different lowercase letters indicate significant differences among the samples in terms of bulk density, flowability and residual water ($p < 0.05$).

	Process Yield (%)	Particle size (μm)				Bulk density ± sd (g/mL)	Flowability	Residual water ± sd (%)
		Dv10	Dv50	Dv90	SPAN		HR ± sd	
P1	86.45	3.57	8.94	19.10	1.74	0.393 ± 0.014^{a}	1.63 ± 0.06^{ab}	7.36 ± 0.56^{ab}
P2	86.37	4.25	11.48	28.01	2.07	0.420 ± 0.015^{a}	1.48 ± 0.05^{a}	7.69 ± 0.51^{ab}
P3	86.62	6.23	14.46	32.05	1.79	0.395 ± 0.014^{a}	1.67 ± 0.06^{b}	8.11 ± 0.76^{a}
P4	88.93	5.98	15.53	42.74	2.37	0.412 ± 0.001^{a}	1.60 ± 0.09^{ab}	6.14 ± 0.73^{b}

2018).

The average diameters of microparticles were higher than those reported in other research works (Bajaj et al., 2021; Bordón et al., 2021a) and this result could be attributable to the higher solid content of the E5 emulsion compared to that of the emulsions proposed by other authors. In general, the particle size of the dried microparticles was higher than those of the oily droplets of the E5 emulsion. This was expected because a single dried particle could entrap, at the same time, more than one oily droplet and this is inevitably responsible for an increase in the particle size. Moreover, as suggested by Bordón et al. (2021b), during the atomization step, the droplet size distribution of the emulsion could change and the original droplets could enlarge and give rise to larger solid particles after drying.

The variation of the process parameters affected the characteristics of the final product (Table 4). Indeed, the progressive increase in the feeding rate was responsible for an increase in the particle dimensions. The average diameters were 10.32 μm for P1, 14.44 μm for P2, 17.24 μm for P3 and 20.58 μm for P4. As reported by Ziaee et al., 2019, when the feed material atomization was carried out increasing the feeding rate, the energies available for the rupture of the material flow were low, and enlarged droplets were formed. As a consequence, they dried into enlarged particles. The SPAN of all the batches of powders, which indicates the width of particle size distribution, was quite high (ranging from 1.74 for P1 to 2.37 for P4) and demonstrated a certain particle size variability. This variability could be explained by the different feeding rates of the product in the trials, which, at the same atomization pressure, could lead to a wider droplet size distribution, resulting in a higher SPAN.

The feeding rate of the emulsion and the T_{in} not affected significantly the bulk density of the final powders. Quite low values of bulk densities characterized P1, P2, P3, and P4 powders (Table 4) even if they are in line with those of spray-dried powders obtained by other authors (Jüptner and Scherließ, 2020; Qadri et al., 2023; Saha et al., 2019). This could be a disadvantage in terms of storage because small amounts of powders require large packaging to be stored. Moreover, a powder with low bulk density could have a large amount of air in the space within particles, which can be responsible for the oxidative degradation of the oil and the consequent reduction of powder stability (Tonon et al., 2011; Linke et al., 2020).

The powders obtained were not fully satisfying in terms of flow attitude (HR values between about 1.5 and 1.7) (Table 4). The poor flowability of a powder is generally due to particles' morphology, small particle size, and high residual moisture content, properties that can be typical of a spray-dried powder obtained using a low T_{in} (Mohammed et al., 2020). The inlet temperatures used in the present work probably were too low to impact positively on the flow properties of the powder. Başyiğit et al. (2020) demonstrated indeed that the powder flowability improved by setting high T_{in} and that the most satisfying results were achieved when T_{in} was 195 °C.

Despite the different feed rate conditions used to obtain P1, P2, and P3 (2.46, 3.70, and 5.46 g/min, respectively), no significant difference in the final moisture content was appreciated (Table 4). Differently, the increase of the T_{in} and the feeding rate at the same time (P4) resulted in slightly lower residual water with a value of about 6 %.

The oil recovered from P1, P2, P3 and P4 powders was between 78 and 90 % of the expected demonstrating that the formulation changes carried out on the preliminary emulsion were successful and confirming the ability of arabic gum to display good carrier behaviour. At the same time, there were slight differences among the samples obtained setting different process parameters. Particularly, the percentages of oil recovered increased according to the following order P1 (78.13 ± 9.22) < P2 (79.10 ± 0.33) < P3 (83.50 ± 1.21) < P4 (89.56 ± 1.75). These results partially confirmed those reported by other authors (Shamaei et al., 2017; Aguiar et al., 2020; Álvarez et al., 2022). Encapsulation efficiency increases when the spray drying treatment is carried out using higher T_{in} because the high temperature of the drying air is responsible for the rapid evaporation of the water present on the droplets' surface and for the quick formation of a hard layer which impedes the oil loss but allows water diffusion. As regards the feeding rate and the encapsulation efficiency, in some research papers (Mousavi Kalajahi and Ghandiha, 2022) it was demonstrated that there was no relationship between them and the obtained results confirmed this thesis.

The residual humidity of the spray-dried powder was crucial to selecting the best process conditions, as it is fundamental to preserve the stability and shelf life of the final product. Thanks to the application of a higher T_{in}, P4 was the most promising powder with the lowest residual water content (6.1 %). Moreover, despite the high T_{in}, the peroxide value of the oil recovered from P4 slightly increased (16.25 ± 1.81) compared to that of the fresh oil (11.37 ± 2.73), without exceeding the limit of acceptability (20 meQ O_2/kg lipid) (Codex Alimentarius, 1999; Gómez-Alonso et al., 2004).

In the second part of the project, E5 emulsion was loaded with vitamin D3. During the spray drying process, an increase of T_{out} (94 °C) was recorded, probably caused by the spray dryer covering, which limited the heat dispersion. The process yield slightly decreased (72.85 %) compared to those obtained in the case of placebo powders, probably because the high temperature reached, close to the glass transition temperature of the excipients, increased the stickiness of the microparticles and, consequently, the loss of the product on the tower walls. The mean oil recovery was 85.69 ± 3.91 %, not so different compared to the result obtained in the case of the corresponding placebo.

The E5-D microparticles were similar to P4 ones in terms of dimensions (23 μm in average diameter, Dv10: 5.83 μm; Dv50: 14.76 μm; Dv90: 51.04 μm; SPAN: 3.06) and extremely poor flow attitude (HR: 1.52 ± 0.04).

Considering the SPE method efficiency (83.6 ± 0.07 %), the vitamin D3 recovered from the microparticles immediately after their preparation was 80.10 ± 9.94 % of the expected and it was higher than that reported by other authors (Bajaj et al., 2021; Tchuenbou-Magaia et al., 2022). Even if there are some authors (Bajaj et al., 2021) who obtained a higher value for entrapment efficiency of vitamin D3, the data are not comparable with those obtained in this work being the determination method of the lipophilic compound indirect and the characteristics of the microparticles very different. A portion of the active compound could be lost during the spray drying process or degraded during the liquid–liquid extraction used to recover the oil from the powder. To prove the selected excipients' ability to protect the active compound, a vitamin D3 oily solution was submitted to a thermal treatment at the same temperature used during the spray drying process. The recovery of vitamin D3 from the oil solution (66.63 ± 1.92 %) was lower than that

from the microparticles, confirming that the compound was preserved when encapsulated into polynucleate microcapsules.

The spray-dried powder was stored under accelerated stability conditions and was submitted to UV-light exposure to evaluate the performance of the selected platform to protect vitamin D3 from degradation. The accelerated stability tests were conducted on E5-D microparticles and vitamin D3 oily solution. As reported in Fig. 4, it can be observed that after six months in the climatic chamber, the microparticles contained more than double vitamin D3 (47.58 ± 6.72 %) compared to the oily solution (20.26 ± 0.16 %). The ability of the spray-dried microparticles proposed in this work to preserve the liposoluble vitamin is in line with that reported by other authors even if different carrier excipients were used to encapsulate vitamin D3 (Bajaj et al., 2021).

Evaluating the UV-stress effect on both samples, the obtained results showed that the difference among the samples was slightly reduced: vitamin D3 was better preserved in the microparticles (64.91 ± 4.29) than in the oily solution (51.34 ± 0.30). Overall, these results demonstrated that vitamin D3 could be better preserved from degradation if encapsulated. Therefore, the selection of adequate carrier excipients able to efficiently retain the sensitive compound combined with the identification of the right process parameters could make spray drying a suitable technique also for microencapsulating thermosensitive active compounds without significantly affecting their stability.

3.3. Pilot-scale spray-dried powders

The principal goal of the trials on the pilot-scale equipment was to preserve the critical quality attributes (CQAs) of microparticles and the physicochemical properties of the loaded oil. For this reason, the most promising results showed by P4 lab-scale spray-dried powder were used as a reference when the pilot-scale spray drying process conditions were set. This target was achieved by exploring the input variables and process conditions. In particular, a comparison was conducted between co-current and counter-current equipment layouts, and for each of them, two different T_{in} were investigated to determine how extended residence time and temperature exposure influenced the final product characteristics.

As an initial strategy for determining the test conditions on the pilot spray dryer, a dimensionless parameter was evaluated (ADP), which considers the ratio between the liquid feed rate to be dried and the drying gas. This parameter is used as a scaling factor that links the mass flow of the product with the drying capacity of the system. When the optimal ratio is identified and maintained across different scales, it should help to preserve CQAs of the final product, ensuring more consistency between lab-scale and larger-scale operations (Milanesi et al., 2022). Starting from these considerations, in this work the pilot-scale process parameters were set up according to those of the P4 lab-scale trial. Since the mass of the drying gas on the Buchi B-290 is not known, the tables reported in the literature were used to estimate the approximate value of 29 kg/h with a resulting ADP value of approximately 0.018 (Milanesi et al., 2022). Considering this indication, the feeding rate was set at 2.7 kg/h and in this way, the ADP value obtained on the pilot-scale was 0.020 and comparable with that of the lab-scale.

The process yield was included between 77 and 91 %; for T1, T2, and B1 batches, the results were not so different from those obtained with a lab-scale machine (T1 = 90.64 %; T2 = 86.59; B1 = 88.04 %). In the case of B2, the lowest yield (76.96 %) was justified by the powder adhesion to the drying tower wall. Moreover, the results showed that in both configurations (top and bottom spray), the lowest values of process yield were obtained with the highest T_{in} (170 °C for top spray and 210 °C for bottom spray), probably because of the starting caramelization of sugar-like components of the formulation (Truong et al., 2005). Instead, keeping the T_{in} at 130 °C when the process is carried out in co-current (top spray), the top and low walls of the tower were clean, the microparticles were perfectly dried, and their easy recovery was responsible for the higher yield.

Taking advantage of the possibility of recording the spray drying process in the pilot spray dryer, the drying performance can be evaluated and discussed in more detail compared to the laboratory scale. From the graph reported in Fig. 5, the spray drying process can be broadly divided into four distinct stages: Starting, Conditioning, Process, and Shutting Down. In the starting stage, the system begins to stabilize as the temperature and gas flow rates increase progressively, preparing the equipment for operation. This is followed by the Conditioning stage, in which critical parameters such as inlet and outlet temperatures, gas flow, and pressures are fine-tuned to achieve steady-state operating conditions. Once these parameters stabilize, the Process stage can begin, and the actual drying of the product occurs. During this step, parameters

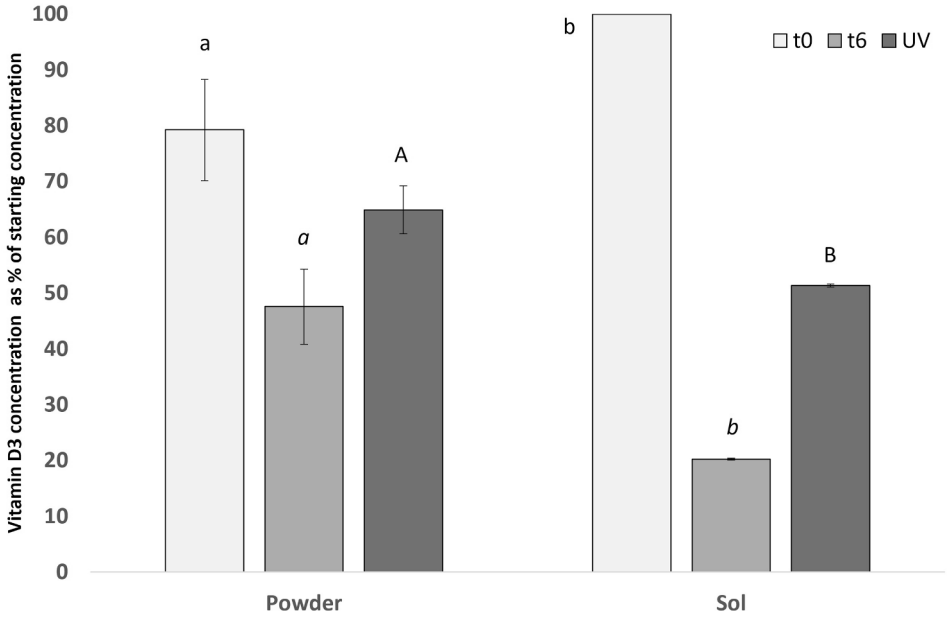

Fig. 4. Influence of storage conditions and UV-light exposure on retention of vitamin D3 in powder and oily solution. Different lowercase letters indicate significant differences among the samples just prepared and used as reference. Different italics letters indicate significant differences among the samples according to accelerated stability conditions ($p < 0.05$), while distinct uppercase letters demonstrate significant differences between the samples at the same UV-light exposure ($p < 0.05$).

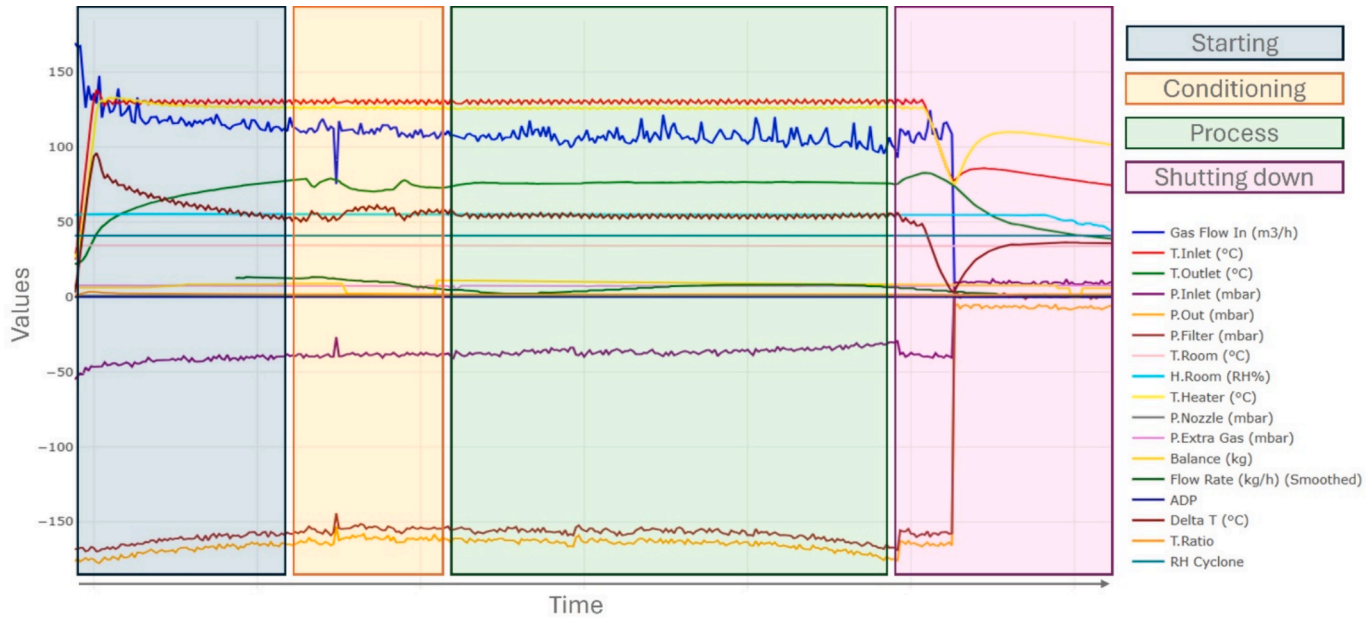

Fig. 5. Variation of the process parameters during the stages of the spray drying process. Highlighted the different stages during the spray drying process: the initial heating (Starting) of the equipment, followed by the conditioning step with the introduction of the solvent. After the outlet temperature is stationary the feed of the product begins (Process phase) and is monitored to maintain constant process conditions until the end of the process since this is the most important part of the final product. The equipment shuts down after the product discharge to avoid possible stress induced by the temperature peak.

like the inlet and outlet air temperatures, pressures, and flow rates must remain consistent, ensuring efficient drying and particle formation. Finally, at the end of the process, the spray dryer enters the Shutting Down stage, during which the decrease in temperatures and pressures is controlled by the software, safely ending the process and ensuring equipment stability post-operation. With this data, it is possible to assess if some events have taken place during the process that compromise the final product quality and results.

The comparison of the four different batches is shown in Fig. 6. The four trials (T1, T2, B1, B2) are presented with a focus on the Process stage using just the critical parameters typically monitored in laboratory-scale spray drying (T_{in}, T_{out}, feed rate/balance, gas flow). The T_{in} (°C) was relatively stable across trials, with a slight fluctuation observed in trial B2, where a temporary drop occurred. This temperature variation could potentially impact the drying rate and product quality. The Gas Flow In (m^3/h) showed similar variation between trials, only B2

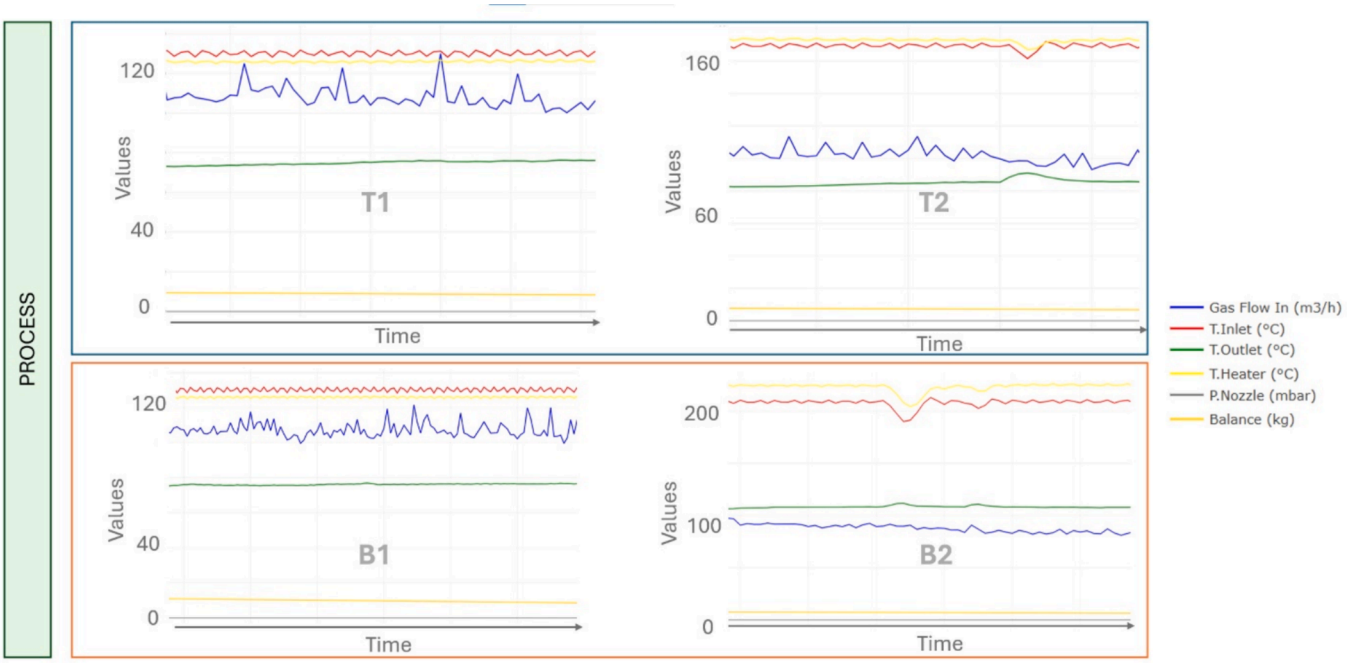

Fig. 6. Focus on the variation of the parameters during the Process stage. Since this step is the one that affects t the final product, a comparison between the 4 different batches was made to identify potential oscillations that could compromise the final powder characteristics. The feeding rate visible using the weight loss of the balance (Orange) remained stable ensuring a continuous atomization. Some increments in the outlet temperature are visible in T2 and B2, in correspondence to oscillations of the heater temperature.

exhibits slightly lower rates, which can be explained by the higher temperature that diminishes the air density and the blower performance, even though the airflow is lower thanks to the higher T_{in} the drying of the product is not affected. Similarly, the Flow Rate (kg/h), a key determinant of drying efficiency, remained constant over the tests.

As expected, the pilot-scale production was successful in terms of residual humidity of the powder compared to the lab-scale treatments (2–3 % *vs* 6–7 %). The significant decrease in residual water content can be attributed to the longer residence time of the microparticles within the larger pilot chamber as well as to the greater efficiency in heat distribution and heat retention thanks to the insulated stainless-steel chamber which can thermally control the internal environment of the tower, thus promoting a lower heat dissipation with faster and complete solvent evaporation (Bordón et al., 2021a).

Another peculiar result is that the residual moisture seems not to be influenced by the temperature variations at the inlet and outlet of the spray drying process; moreover, the lower or upper spray configuration also seems to have a limited effect on the final moisture, despite the different thermal stress of these two configurations. A possible explanation is that the product's moisture content may reach a dynamic equilibrium, where further moisture removal becomes increasingly difficult regardless of the variations in inlet and outlet temperatures. This can occur due to the rapid initial evaporation of free moisture, which dominates the drying process. As the product reaches a low moisture state, the rate of evaporation significantly decreases, particularly when bound or adsorbed water remains. At this stage, the drying rate is governed by the slow diffusion of residual moisture within the particles, resulting in a similar final moisture content despite changes in drying conditions. This observation appears to be in line with laboratory tests where changes in feed rate did not result in a significant reduction of the final moisture content, suggesting that the drying dynamics are not substantially affected by the feed rate and supporting the idea that the process becomes limited by internal moisture diffusion rather than external drying conditions. Compared to the powders collected from the lab-scale spray dryer, in the case of the pilot-scale production, the particle dimensions increased mainly because of the difference in the amount of feed per unit of time and atomization devices/conditions. In detail, the average diameter was at least five times that of P4 microparticles, and the particle size distribution was not narrow (Table 5).

By modifying the layout and maintaining unchanged process conditions (T1 *vs* B1), when the bottom spray configuration was used the size of microparticles significantly increased due to the high probability of microparticles aggregation in the counter-current flow (Table 5). In this case, as Piatkowski and Zbicinski, 2007 reported, the collision between the just-dried small microparticles and the droplets of feed emulsions is responsible for the formation of agglomerates that, moving in the tower, come into contact with other feed droplets and increase their dimensions. This process goes on until the aerodynamic resistance of hot air flow becomes less than the gravity force on the agglomerates, which can be recovered.

Moreover, the obtained results evidenced that the different T_{in} selected for the top and bottom spray had different effects on the dimensions of microparticles: the Dv90 of top-sprayed powders (T1 and T2) was similar, while in the case of the bottom-sprayed powder, the Dv90 of B1 (low T_{in}) was double that of B2 (high T_{in}).

The bulk densities of the pilot-scale spray-dried powders were low and in the same range as those of the lab-scale products. The lower bulk density was due to the high T_{in} associated with the bottom spray configuration, which confirms the lower aggregation occurred during the drying process (Table 5).

The change in spray drying equipment (from lab-scale to pilot scale) and process conditions did not improve the flowability characteristics of the powders, which were always not satisfying. As expected, the B2 sample composed of microparticles with the lowest average diameter showed the worst results. In this case, the cohesive forces among small particles impeded their flowability. Shamaei et al. (2017) demonstrated that an increase in the T_{in}, the residual humidity content of microparticles, and their irregular shape are responsible for a decrease in powder bulk density and a worsening of their flow properties. For this reason, being the results of the present work in contrast with the literature, further studies will be carried out to investigate deeply this aspect.

SEM images show the typical particle size characteristic of spray-dried powders, that is the presence of microparticles of different dimensions (Fig. 7). Microparticles had a spherical shape and an irregular but continuous surface without cracks or holes. This means that they were not permeable to gases, ensuring the efficient retention of the oil droplets. The structure collapsed with shrinkage due to water evaporation, presenting some surface depressions probably attributable to the presence of viscoelastic wall materials, the evaporation rate, or the atomization method (Bordón et al., 2021a; Brytan et al., 2025). Moreover, the wall of the microparticles showed the lipophilic material distributed as small droplets embedded in the polymeric matrix.

Oil recovery increased compared to lab-scale tests, ranging from 87 % to 98 % of the expected. In general, the larger size of the pilot scale spray-dried particles seems to have improved their ability to entrap the oil droplets, confirming that the larger the particle size, the higher the content of carrier excipients as well as the lipophilic core in the same generated droplet. It is also interesting to evidence that, if in the case of the top-spray layout the best oil encapsulation efficiency was obtained with the lowest T_{in} (97 % *vs* 89 %), for the bottom spray the higher T_{in} favored the oil loading (98 % *vs* 87 %).

The peroxide values of the oil recovered from T1, T2, B1 and B2 powders were determined to evaluate if the selected process conditions were stressful. Immediately after the preparation, the T1 and B1 samples showed a low oxidation level compared to the fresh oil (that is the non-treated oil used as reference, NT-oil), while T2 and B2 were characterized by peroxide values near or over the acceptability limit. In the case of bottom sprayed powders, regardless of T_{in}, high standard deviations are indicative of the lack of sample homogeneity due to stochastic interaction and agglomeration along with a higher residence time during the drying process. This result is in line with the type of equipment and its configuration. To guarantee good process yields, in general, the pilot-scale spray dryer requires the treatment of large amounts of feed material. Once dried, the particles remain in the machine until all the feed material is processed. This extra-exposure time to heat could be responsible for the reduction in their quality. The additional exposure time is not the same for all the particles, but it is longer for those that were dried at the initial phase of the process. This aspect is more evident in the counter-current configuration because it exposes the already dried microparticles to high temperatures. According to the data collected, the

Table 5
Characteristics of pilot-scale spray-dried powders. Different lowercase letters indicate significant differences among the samples in terms of bulk density, flowability and residual water ($p < 0.05$).

	Particle size				Bulk density ± sd (g/mL)	Flowability	Residual water ± sd (%)
	Dv10	Dv50	Dv90	SPAN		HR ± sd	
T1	9.88	34.80	105.70	2.75	0.373 ± 0.011^{a}	1.79 ± 0.05^{ab}	3.13 ± 0.38^{a}
T2	11.51	36.70	114.00	2.79	0.368 ± 0.030^{a}	1.71 ± 0.07^{ab}	2.98 ± 0.38^{a}
B1	13.37	55.60	170.20	2.82	0.423 ± 0.020^{a}	1.66 ± 0.10^{a}	3.33 ± 0.57^{a}
B2	10.69	32.05	95.53	2.65	0.302 ± 0.029^{b}	1.92 ± 0.14^{b}	2.76 ± 1.07^{a}

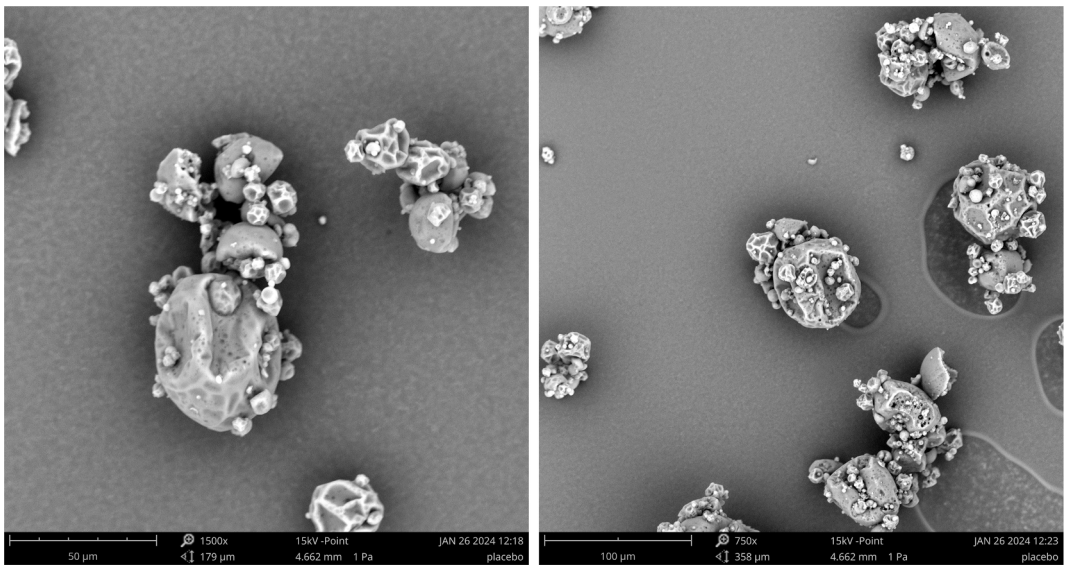

Fig. 7. SEM images of the microparticles obtained by the T1 spray drying process.

top-spray set-up and the lower T_{in} were the optimal combinations to preserve the stability of the oily cores.

After six months of storage at room temperature, the oxidation state of the oil encapsulated was evaluated again. The peroxide values increased over time for all the samples tested (Fig. 8): in the case of free oil, oxidation was almost eight times higher while the results obtained for the powders were promising, given a not-so-drastic worsening of the quality of oil after a long storage period. The oxidative stability of the powders could be influenced not only by the combination of the carrier excipients and the oil droplets distribution in the polymeric matrix but also by the potential antioxidant activity associated with the pea protein hydrolysate. Indeed, in general, proteins could prevent the oxidation of oil-in-water emulsions thanks to their ability in metal chelation and free radical scavenging (Tamm et al., 2016). With this aim, the milky protein was extremely studied, but it was demonstrated that pea protein hydrolysates also have similar properties improved by enzymatic hydrolysis (Tamm et al., 2016).

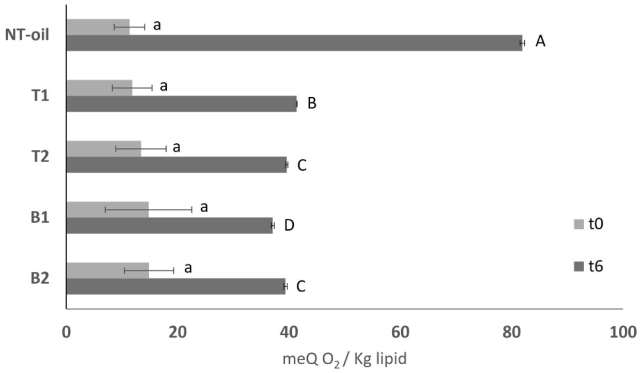

Fig. 8. Peroxide value of non-treated oil (NT-oil) compared to T1, T2, B1 and B2 tests from pilot-scale spray dryer just prepared (t0) and after six-months (t6). Different lowercase letters indicate significant differences among the samples just prepared ($p < 0.05$), while distinct uppercase letters demonstrate significant differences between the samples after six months of storage ($p < 0.05$).

4. Conclusion

Polynucleate microcapsules have been produced by emulsification and spray drying: lipophilic compartments loaded with vitamin D3 have been embedded in a micrometric hydrophilic matrix able to efficiently preserve the active compound. The pea protein hydrolysate was demonstrated to be a promising natural emulsifier if combined with excipients displaying a suitable carrier behavior, able to retain the oil droplets better into the microparticle structure. At the same time, the selection of the spray drying process parameters influenced the quality of the final product and its stability.

Therefore, this study highlights the critical interdependence between formulation and process parameters in spray drying. The findings underscore that without a well-designed formulation, encapsulation efficiency may be compromised, and without careful optimization of process parameters, the stability and quality of the encapsulated compound may not be maintained.

Funding sources

The present work is part of the project "VITADWASTE—Innovative and sustainable processes for the development of Vitamin D nutraceutical from fish waste: extraction, formulation and clinical study for the evaluation of its bioavailability and clinical equivalence" funded by MIUR—Ministero dell'Istruzione dell'Università e della Ricerca—PRIN: Progetti di Ricerca di Rilevante Interesse Nazionale, Bando 2022. Project code: 2022M9JL3T.

Credit author statement

Giada Diana: Methodology, Formal analysis, Investigation, Data curation, Writing original. **Andrea Milanesi:** Methodology, Formal analysis, Investigation, Data curation, Writing original. **Alessandro Candiani:** Investigation, Visualization, Writing revision. **Alessandro Sodano:** Investigation. **Paolo Rassè:** Investigation. **Andrea Foglio Bonda:** Writing revision, Supervision. **Laura Alessandroni:** Investigation, Writing revision. **Lorella Giovannelli:** Conceptualization, Resources, Writing revision, Supervision. **Lorena Segale:** Conceptualization, Methodology, Resources, Writing revision, Supervision, Project administration. **Jean Daniel Coisson:** Conceptualization, Resources, Writing revision, Funding, Project administration.

Declaration of competing interest

The authors declare that they have no known competing financial interests or personal relationships that could have appeared to influence the work reported in this paper.

Acknowledgements

The authors thank A. Costantino S.p.A. (Favria – TO, Italy) for kindly donating pea protein hydrolysate.

Data availability

The authors are unable or have chosen not to specify which data has been used.

References

Aguiar, M.C.S., das Graças Fernandes da Silva, M.F., Fernandes, J.B., Forim, M.R., 2020. Evaluation of the microencapsulation of orange essential oil in biopolymers by using a spray-drying process. Sci Rep 10. https://doi.org/10.1038/s41598-020-68823-4.

Al-Khattawi, A., Bayly, A., Phillips, A., Wilson, D., 2018. The design and scale-up of spray dried particle delivery systems. Expert Opin Drug Deliv. https://doi.org/10.1080/17425247.2017.1321634.

Álvarez, R., Giménez, B., Mackie, A., Torcello-Gómez, A., Quintriqueo, A., Oyarzun-Ampuero, F., Robert, P., 2022. Influence of the particle size of encapsulated chia oil on the oil release and bioaccessibility during in vitro gastrointestinal digestion. Food Funct 13, 1370–1379. https://doi.org/10.1039/d1fo03688b.

Bajaj, S.R., Marathe, S.J., Singhal, R.S., 2021. Co-encapsulation of vitamins B12 and D3 using spray drying: Wall material optimization, product characterization, and release kinetics. Food Chem 335. https://doi.org/10.1016/j.foodchem.2020.127642.

Başyiğit, B., Sağlam, H., Kandemir, Ş., Karaaslan, A., Karaaslan, M., 2020. Microencapsulation of sour cherry oil by spray drying: Evaluation of physical morphology, thermal properties, storage stability, and antimicrobial activity. Powder Technol 364, 654–663. https://doi.org/10.1016/j.powtec.2020.02.035.

Bordón, M.G., Paredes, A.J., Camacho, N.M., Penci, M.C., González, A., Palma, S.D., Ribotta, P.D., Martinez, M.L., 2021a. Formulation, spray-drying and physicochemical characterization of functional powders loaded with chia seed oil and prepared by complex coacervation. Powder Technol 391. https://doi.org/10.1016/j.powtec.2021.06.035.

Bordón, M.G., Alasino, N.P.X., Villanueva-Lazo, Á., Carrera-Sánchez, C., Pedroche-Jiménez, J., Millán-Linares, M. del C., Ribotta, P.D., Martínez, M.L., 2021b. Scale-up and optimization of the spray drying conditions for the development of functional microparticles based on chia oil. Food Bioprod. Process. 130, 48–67. https://doi.org/10.1016/j.fbp.2021.08.006.

Brytan, W., Amorim, R., Padrela, L., 2025. Process control and design of drying technologies for biopharmaceuticals – A review. Powder Technol. https://doi.org/10.1016/j.powtec.2024.120395.

Camacho-Lie, M., Antonio-Gutiérrez, O., López-Díaz, A.S., López-Malo, A., Ramírez-Corona, N., 2023. Factors influencing droplet size in pneumatic and ultrasonic atomization and its application in food processing. Discover Food. https://doi.org/10.1007/s44187-023-00065-5.

Candiani, A., Diana, G., Martoccia, M., Travaglia, F., Giovannelli, L., Coïsson, J.D., Segale, L., 2023. Microencapsulation of a Pickering Oil/Water Emulsion Loaded with Vitamin D3. Gels 9. https://doi.org/10.3390/gels9030255.

Carmona, P.A.O., Garcia, L.C., Ribeiro, J.A. de A., Valadares, L.F., Marçal, A. de F., de França, L.F., Mendonça, S., 2018. Effect of Solids Content and Spray-Drying Operating Conditions on the Carotenoids Microencapsulation from Pressed Palm Fiber Oil Extracted with Supercritical CO2. Food Bioproc Tech 11, 1703–1718. DOI: 10.1007/s11947-018-2132-3.

Carneiro, H.C.F., Tonon, R.V., Grosso, C.R.F., Hubinger, M.D., 2013. Encapsulation efficiency and oxidative stability of flaxseed oil microencapsulated by spray drying using different combinations of wall materials. J Food Eng 115. https://doi.org/10.1016/j.jfoodeng.2012.03.033.

Codex Alimentarius, 1999. Standard for Named Vegetable Oils Codex Stan 210-1999; Adopted in 1999. Revision: 2001, 2003, 2009. Amendment: 2005, 2011, 2013 and 2015. Codex Alimentarius.

Council of Europe - EDQM, 2023. European Pharmacopoeia 11th Edition, Oak Bark.

Dima, C., Milea, A.S., Constantin, O.E., Stoica, M., Stela Ivan, A., Alexe, P., Stanciuc, N., 2020. Fortification of pear juice with vitamin D3 encapsulated in polymer microparticles: physico-chemical and microbiolgical characterization. journal-of-agroalimentary.roC Dima, AS Milea, OE Constantin, M Stoica, AS Ivan, P Alexe, N StanciucJ. Agroaliment. Process Technol, 2020•journal-of-agroalimentary.ro 26.

Esposito, T., Mencherini, T., Del Gaudio, P., Auriemma, G., Franceschelli, S., Picerno, P., Aquino, R.P., Sansone, F., 2020. Design and development of spray-dried microsystems to improve technological and functional properties of bioactive compounds from hazelnut shells. Molecules 25. https://doi.org/10.3390/molecules25061273.

Gómez-Alonso, S., Mancebo-Campos, V., Salvador, M.D., Fregapane, G., 2004. Oxidation kinetics in olive oil triacylglycerols under accelerated shelf-life testing (25-75°C). Eur. J. Lipid Sci. Technol. 106. https://doi.org/10.1002/ejlt.200300921.

Gonçalves, A., Estevinho, B.N., Rocha, F., 2022. Spray-drying of oil-in-water emulsions for encapsulation of retinoic acid: Polysaccharide- and protein-based microparticles characterization and controlled release studies. Food Hydrocoll 124. https://doi.org/10.1016/j.foodhyd.2021.107193.

ICH Topic Q 1 A (R2) Stability Testing of new Drug Substances and Products Step 5 NOTE FOR GUIDANCE ON STABILITY TESTING: STABILITY TESTING OF NEW DRUG SUBSTANCES AND PRODUCTS, 2003.

ICH Topic Q1B Photostability Testing of New Active Substances and Medicinal Products Step 5 NOTE FOR GUIDANCE ON THE PHOTOSTABILITY TESTING OF NEW ACTIVE SUBSTANCES AND MEDICINAL PRODUCTS, 1998.

Jüptner, A., Scherließ, R., 2020. Spray dried formulations for inhalation—meaningful characterisation of powder properties. Pharmaceutics 12. https://doi.org/10.3390/pharmaceutics12010014.

Linke, A., Hinrichs, J., Kohlus, R., 2020. Impact of the powder particle size on the oxidative stability of microencapsulated oil. Powder Technol 364. https://doi.org/10.1016/j.powtec.2020.01.077.

Maurya, V.K., Bashir, K., Aggarwal, M., 2020. Vitamin D microencapsulation and fortification: Trends and technologies. J. Steroid Biochem. Mol. Biol. https://doi.org/10.1016/j.jsbmb.2019.105489.

Milanesi, A., Rizzuto, F., Rinaldi, M., Foglio Bonda, A., Segale, L., Giovannelli, L., 2022. Thermodynamic Balance vs. Computational Fluid Dynamics Approach for the Outlet Temperature Estimation of a Benchtop Spray Dryer. Pharmaceutics 14. https://doi.org/10.3390/pharmaceutics14020296.

Mohammed, N.K., Tan, C.P., Manap, Y.A., Muhialdin, B.J., Hussin, A.S.M., 2020. Spray Drying for the Encapsulation of Oils—A Review. Molecules. https://doi.org/10.3390/molecules25173873.

Mousavi Kalajahi, S.E., Ghandiha, S., 2022. Optimization of spray drying parameters for encapsulation of Nettle (Urtica dioica L.) extract. LWT 158. https://doi.org/10.1016/j.lwt.2022.113149.

O'Sullivan, J.J., Norwood, E.A., O'Mahony, J.A., Kelly, A.L., 2019. Atomisation technologies used in spray drying in the dairy industry: A review. J Food Eng. https://doi.org/10.1016/j.jfoodeng.2018.08.027.

Pacheco-Quito, E.M., Ruiz-Caro, R., Veiga, M.D., 2020. Carrageenan: Drug delivery systems and other biomedical applications. Mar Drugs. https://doi.org/10.3390/md18110583.

Piatkowski, M., Zbicinski, I., 2007. Analysis of the mechanism of counter-current spray drying. Transp Porous Media 66, 89–101. https://doi.org/10.1007/s11242-006-9024-0.

Pludowski, P., Grant, W.B., Karras, S.N., Zittermann, A., Pilz, S., 2024. Vitamin D Supplementation: A Review of the Evidence Arguing for a Daily Dose of 2000 International Units (50 μg) of Vitamin D for Adults in the General Population. Nutrients. https://doi.org/10.3390/nu16030391.

Poozesh, S., Bilgili, E., 2019. Scale-up of pharmaceutical spray drying using scale-up rules: A review. Int J Pharm. https://doi.org/10.1016/j.ijpharm.2019.03.047.

Qadri, T., Naik, H.R., Hussain, S.Z., Bhat, T.A., Naseer, B., Zargar, I., Beigh, M.A., 2023. Impact of spray drying conditions on the reconstitution, efficiency and flow properties of spray dried apple powder-optimization, sensorial and rheological assessment. Heliyon 9. https://doi.org/10.1016/j.heliyon.2023.e18527.

Sablania, V., Bosco, S.J.D., 2018. Optimization of spray drying parameters for Murraya koenigii (Linn) leaves extract using response surface methodology. Powder Technol 335. https://doi.org/10.1016/j.powtec.2018.05.009.

Saha, D., Nanda, S.K., Yadav, D.N., 2019. Optimization of spray drying process parameters for production of groundnut milk powder. Powder Technol 355. https://doi.org/10.1016/j.powtec.2019.07.066.

Salama, A.H., 2020. Spray drying as an advantageous strategy for enhancing pharmaceuticals bioavailability. Drug Deliv Transl Res. https://doi.org/10.1007/s13346-019-00648-9.

Shamaei, S., Seiiedlou, S.S., Aghbashlo, M., Tsotsas, E., Kharaghani, A., 2017. Microencapsulation of walnut oil by spray drying: Effects of wall material and drying conditions on physicochemical properties of microcapsules. Innov. Food Sci. Emerg. Technol. 39, 101–112. https://doi.org/10.1016/j.ifset.2016.11.011.

Tamm, F., Herbst, S., Brodkorb, A., Drusch, S., 2016. Functional properties of pea protein hydrolysates in emulsions and spray-dried microcapsules. Food Hydrocoll 58, 204–214. https://doi.org/10.1016/j.foodhyd.2016.02.032.

Tchuenbou-Magaia, F.L., Tolve, R., Anyadike, U., Giarola, M., Favati, F., 2022. Co-encapsulation of vitamin D and rutin in chitosan-zein microparticles. J. Food Meas. Charact. 16. https://doi.org/10.1007/s11694-022-01340-2.

Terracina, F., Caruana, R., Bonomo, F.P., Montalbano, F., Licciardi, M., 2022. Gastro-Resistant Microparticles Produced by Spray-Drying as Controlled Release Systems for Liposoluble Vitamins. Pharmaceutics 14. https://doi.org/10.3390/pharmaceutics14071480.

Tonon, R.V., Grosso, C.R.F., Hubinger, M.D., 2011. Influence of emulsion composition and inlet air temperature on the microencapsulation of flaxseed oil by spray drying. Food Res. Int. 44, 282–289. https://doi.org/10.1016/j.foodres.2010.10.018.

Truong, V., Bhandari, B.R., Howes, T., 2005. Optimization of co-current spray drying process of sugar-rich foods. Part I-Moisture and glass transition temperature profile during drying. J Food Eng 71. https://doi.org/10.1016/j.jfoodeng.2004.10.017.

van Boven, A.P., Eijkelboom, N.M., Fentsahm, K.J., Gruson, M.J., Boom, R.M., Wilms, P. F.C., Kohlus, R., Schutyser, M.A.I., 2024. A multiscale investigation on protein addition toward steering agglomeration and yield in spray drying. LWT 212. https://doi.org/10.1016/j.lwt.2024.116998.

Ziaee, A., Albadarin, A.B., Padrela, L., Femmer, T., O'Reilly, E., Walker, G., 2019. Spray drying of pharmaceuticals and biopharmaceuticals: Critical parameters and experimental process optimization approaches. Eur. J. Pharm. Sci. https://doi.org/10.1016/j.ejps.2018.10.026.